



Norwegian University of  
Science and Technology

# Vurdering av beregningsmetoder for vind-karakteristika

**Anja Eide Onstad**

Master of Energy and Environmental Engineering

Submission date: June 2016

Supervisor: Lars Sætran, EPT

Norwegian University of Science and Technology  
Department of Energy and Process Engineering



EPT-M-2016-96

**MASTER THESIS**

for

Student  
Anja Eide Onstad

Spring 2016

Evaluation of methods for prediction of wind characteristics

*Vurdering av beregningsmetoder for vind-karakteristikka*

The *Recommended Practice DNV-RP-C205 “Environmental conditions and environmental loads” (2007)* (RP) gives guidance for modeling, analysis and prediction of environmental conditions as well guidance for calculating environmental loads acting on structures. The loads are limited to those due to wind, wave and current. The RP is based on state of the art within modeling and analysis of environmental conditions and loads and technical developments in recent R&D projects, as well as design experience from recent and ongoing projects. The basic principles applied in the RP are in agreement with the most recognized rules and reflect industry practice and latest research.

We are for this thesis work focusing on wind. Wind that varies in time and space and is characterized by statistical moments, gust factors and spectra. Modeling, analysis and prediction of environmental conditions are important for calculating wind loads on structures. Some of the prediction methods are presented in the above mentioned RP. We have access to several years of wind data from the met-station at Titran, Frøya. This data bank enables an opportunity to test and evaluate prediction methods for wind conditions – methods that are presented in the reference above and/or can be found in the research literature.

Within 14 days of receiving the written text on the master thesis, the candidate shall submit a research plan for his project to the department.

When the thesis is evaluated, emphasis is put on processing of the results, and that they are presented in tabular and/or graphic form in a clear manner, and that they are analyzed carefully.

The thesis should be formulated as a research report with summary both in English and Norwegian, conclusion, literature references, table of contents etc. During the preparation of the text, the candidate should make an effort to produce a well-structured and easily readable report. In order to ease the evaluation of the thesis, it is important that the cross-references are correct. In the making of the report, strong emphasis should be placed on both a thorough discussion of the results and an orderly presentation.

The candidate is requested to initiate and keep close contact with his/her academic supervisor(s) throughout the working period. The candidate must follow the rules and regulations of NTNU as well as passive directions given by the Department of Energy and Process Engineering.

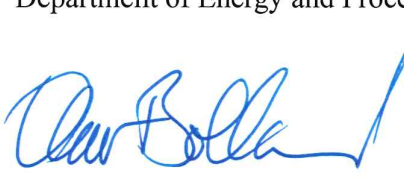
Risk assessment of the candidate's work shall be carried out according to the department's procedures. The risk assessment must be documented and included as part of the final report. Events related to the candidate's work adversely affecting the health, safety or security, must be documented and included as part of the final report. If the documentation on risk assessment represents a large number of pages, the full version is to be submitted electronically to the supervisor and an excerpt is included in the report.

Pursuant to “Regulations concerning the supplementary provisions to the technology study program/Master of Science” at NTNU §20, the Department reserves the permission to utilize all the results and data for teaching and research purposes as well as in future publications.

The final report is to be submitted digitally in DAIM. An executive summary of the thesis including title, student’s name, supervisor's name, year, department name, and NTNU's logo and name, shall be submitted to the department as a separate pdf file. Based on an agreement with the supervisor, the final report and other material and documents may be given to the supervisor in digital format.

- Work to be done in lab (Water power lab, Fluids engineering lab, Thermal engineering lab)
- X  Field work

Department of Energy and Process Engineering, 13. January 2016



Olav Bolland  
Department Head



Lars Sætran  
Academic Supervisor

# Evaluation of methods for prediction of wind characteristics

Anja Eide Onstad

Department of Energy and Process Engineering  
Norwegian University of Science and Technology

June 11, 2016

**Abstract**—Atmospheric stability is important to, among other things, obtain a more accurate estimate of the wind speed profile. This work presents atmospheric stability distributions at two sites from three masts and compares them. Two of the masts are only 3 kilometers apart and their stability distributions are found to be correlated. The atmospheric stability is calculated using the bulk Richardson number, the surface Richardson number and the sonic method. It is shown that the resulting distributions vary depending on which method is utilized.

**Keywords**—Atmospheric stability, Obukhov length, Richardson Gradient, Site correlation comparison

## I. INTRODUCTION

Research shows that accounting for atmospheric stability when estimating the wind speed profile increases the accuracy of the estimation [1]–[3]. The stability conditions at a wind farm site will influence the mean wind profile, turbulence conditions and possibly the wake effects within the wind farm [4]. Atmospheric stability also influences urban pollution [5] and has a general geophysical significance [6].

In an unstable atmosphere there is a large generation rate of turbulence caused by a positive heat flux due to the underlying surface being warmer than the air. When the surface is colder than the air, in a stable atmosphere, it tends to reduce turbulence with a negative heat flux directed downwards. During such conditions, mechanical shear stress is often the only producer of turbulence. If the vertical heat flux is near zero, or much smaller than the mechanical shear stress, the atmosphere is said to be neutral.

This work aims to present atmospheric stability distributions at two different sites and to examine if there is a correlation between the distributions. Especially interesting is the correlation between two masts at the Roan site, located 3 km apart and under similar roughness conditions. In the literature, no preferred method is defined for calculating atmospheric stability and it is left to each researcher how to choose the best method. At the sites included in this study, data from masts with both 2D- and 3D-sonic sensors were available, enabling the comparison of using different expressions of the Richardson number and a sonic method to calculate atmospheric stability.

## II. NOMENCLATURE

$f$	Coriolis parameter
$g$	Acceleration of gravity
$\kappa$	Von Karman constant
$L$	Obukhov length
$P$	Pressure
$P_0$	Reference pressure
$r$	Mixing ratio for unsaturated air
$\rho$	Density
$u$	Wind speed
$u_*$	Friction velocity
$T$	Temperature
$\theta_v$	Virtual potential temperature
$\tau$	Turbulent friction
$\overline{w'T'}$	Temperature flux
$z$	Height
$z_m$	Geometric mean height
$z_{sl}$	Surface boundary layer height
$z_0$	Roughness length

Overbar denotes mean values and an apostrophe denotes fluctuations.

## III. METHODOLOGY

Atmospheric stability is described in Monin-Obukhov theory [6] with the Obukhov length scale  $L$  as the stability parameter. Three different ways to derive this parameter are considered; the bulk Richardson method, the surface Richardson method and the Sonic method, which are explained in detail below.

1) *The Bulk Richardson method*:  $L$  is derived via the bulk Richardson number from the temperature and wind speed measurements at two different heights. The definition from Arya [7] is used when calculating the bulk Richardson number

$$Ri_{bulk} = \frac{g}{\theta_v} \frac{\Delta \bar{\theta}_v z_m}{(\Delta \bar{u})^2} \ln\left(\frac{z_2}{z_1}\right), \quad (1)$$

which is applicable at the geometric mean height  $z_m = \sqrt{z_1 z_2}$ . The virtual potential temperature,  $\theta_v$ , is calculated from:

$$\theta_v = T \frac{1 + \frac{r}{0.622}}{1 + r} \left(\frac{P_0}{P}\right)^{2/7}, \quad (2)$$

where  $P_0$  is a reference pressure of 1 atm. In a virtual potential temperature, temperature variations in the atmosphere caused by changes in pressure and humidity

are removed, meaning that any additional differences in temperature are attributed to difference in heat content [8], [9].

2) *The Surface Richardson method*:  $L$  is calculated from the surface Richardson number as the difference between wind and temperature measurements at a height and ground level. For calculating the surface Richardson number, Byun's [10] definition is used

$$Ri_{surface} = \frac{g}{\theta_v} \frac{\Delta\bar{\theta}_v z}{\bar{u}^2} \ln\left(\frac{z}{z_0}\right), \quad (3)$$

which is applicable at the geometric mean height  $z_m = \frac{z_2}{2}$ .

The findings of Dyer [11] and Businger et al. [12], in accordance with the recommendations of DNV [13], are used when calculating  $L$  from both the bulk Richardson and the surface Richardson number:

$$L = \begin{cases} \frac{z_m}{Ri}, & Ri < 0 \\ \frac{z_m}{Ri}(1 - 5Ri), & 0 < Ri < 0.2. \end{cases} \quad (4)$$

3) *Sonic method*:  $L$  is derived from sonic anemometer measurements of turbulent fluxes

$$L_{sonic} = -\frac{u_*^3}{\kappa w' T'} \frac{\bar{T}}{g}, \quad (5)$$

where the friction velocity is calculated from  $u_* = (\overline{u'w'^2} + \overline{v'w'^2})^{1/4}$ , in accordance with the findings of Weber [14].

#### A. Dividing into stability classes

The derived values of the Obukhov lengths are related to stability classes as defined below:

Very Stable	$0 < L < 200$
Stable	$200 < L < 500$
Neutral	$ L  > 500$
Unstable	$-500 < L < -200$
Very unstable	$-200 < L < 0$ .

## IV. MEASUREMENT SITES



Fig. 1. Map showing the location of the measuring masts at Frøya and Roan.

TABLE I. MAST INSTRUMENTATION, ACCURACIES AND AT WHICH HEIGHT EACH INSTRUMENT IS MOUNTED

	Instrumentation	Accuracy	Heights
Roan327 and Roan328	Thies First Class Advanced Anemometer	< 1%	20, 40, 60, 80 and 100 m (x2)
	Galltec Mess KP Temperature Sensor	$\pm 0.2K$	3 and 97 m
	3D Ultrasonic Thies Sonic Anemometer	2%	98 m
Frøya	Gill WindObserver II 2D Anemometer	$\pm 2\%^1$	Pairs at 10, 16, 25, 40, 70 and 100 m
	Campbell Scientific 109 Temperature Sensor	$\pm 0.25^\circ C^2$	0.2, 10, 16, 25, 40, 70 and 100 m

The sites Frøya and Roan are located on the coast of mid-Norway in the county Sør-Trøndelag as indicated in Figure 1. The mast at Frøya is located approximately 110 km south west from the two masts at Roan which are 3 km apart. In Table I the instrumentation of each mast is given with their respective accuracies, and at which height each instrument is mounted. The two masts at Roan are equally equipped. The mean wind speeds and temperatures at each site are given in Table II.

TABLE II. THE MEASURED MEAN WIND SPEEDS AND TEMPERATURES AT THE SITES

Site	$\bar{u}$ (100 m)	$\bar{T}_1$	$\bar{T}_2$
Frøya	10.1 m/s	281.69 K (10 m)	280.72 K (100 m)
Roan 327	9.5 m/s	279.21 K (3 m)	278.11 K (97 m)
Roan 328	8.9 m/s	279.98 K (3 m)	278.92 K (97 m)

#### A. Frøya Measurement Site

The measuring mast is located on the south-west tip of the Frøya island which is exposed to winds both from the Norwegian sea and the mainland. The mast is located approximately 20 m above sea level and is 100 m high. Pressure and humidity are not measured at the actual site, so data from the nearby meteorological station Sula are used for this. The station at Sula is located on an island approximately 20 km north-east of Frøya.

Approximately 3.5 years of data are available from Frøya. Figure 2 shows the wind rose at the site with a majority of the wind coming either from south-west or north-east, parallel to the shore line. The distance to the sea is different in each direction sector, and is between 500 m and 3 km in the main wind direction with the strongest wind speeds, south-west. The landscape at the site is relatively flat and there are no nearby obstacles that influence the wind measurements. The roughness length is divided into 4 sectors in accordance with the work of Fechner [3]. A more thorough description and assessment of this site is offered by Øistad [15].

#### B. Roan Measurement Site

At Roan, measurements from two 100 m high masts are available. They are located approximately 3 km apart

<sup>1</sup>(> 5m/s)  
<sup>2</sup>(-10 to 70°C)

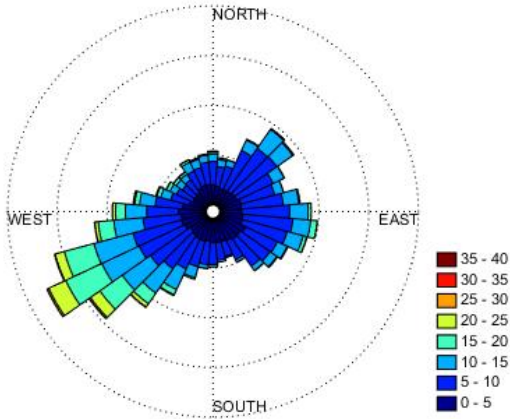


Fig. 2. Wind rose from Frøya at 100 m height, the colors indicate wind speed (m/s) given in the legend to the right.

in a mountainous open area, classified by the Norwegian Mapping Authority [16]. The Norwegian Water Resources and Energy Directorate [17] assigns a roughness length of  $z_0 = 0.03$  m for bare mountains, which is the value applied in all direction sectors for the two masts at Roan. The topography around the masts is shown in Figure 3.

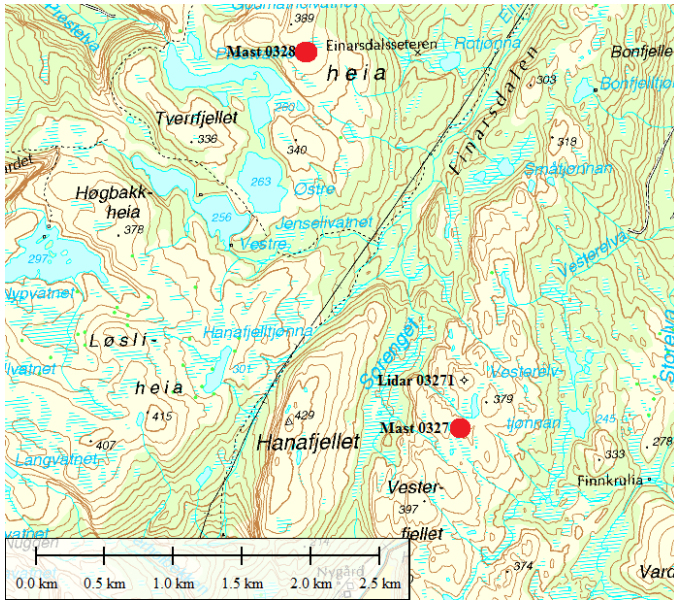


Fig. 3. Map showing the topography around the Roan masts, marked with red dots. Image reproduced with permission of the rights holder, Meventus.

1) *Roan 327*: This mast is located on a peak in a mountainous area at an elevation of 365 m, and Figure 4 displays its wind rose. The distance to the sea in the main wind direction, west, is 7.5 - 9.5 km while the wind from the other main wind direction, south-east, comes from land. Approximately one year of data is available from Roan 327 and the sonic anemometer performed measurements from March 14 2015 until December 5 2015.

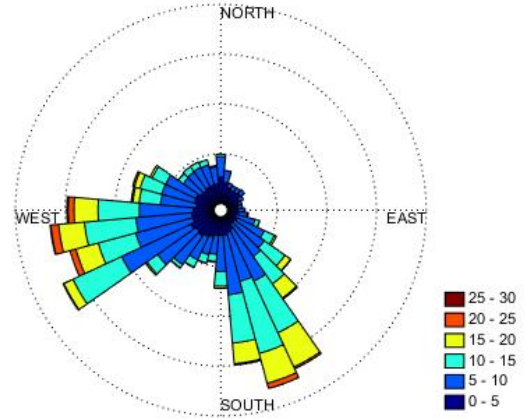


Fig. 4. Wind rose from Roan 327 at 100 m height, the colors indicate wind speed (m/s) given in the legend to the right.

2) *Roan328*: This mast is located at an elevation of 365 m, near the peak of a mountainous area. The wind rose in Figure 5 shows that winds from south-east are less frequent here than at Roan 327. The distance to the sea in the main wind direction, west, is around 6 km, when sea is defined as being outside two small islands that are coupled to land. In the other main wind direction, south-east, the wind has travelled over land. Approximately one year of data is available, while the sonic anemometer only performed measurements for 1.5 months, from April 15 2015 until May 31 2015, before it was struck by lightning.

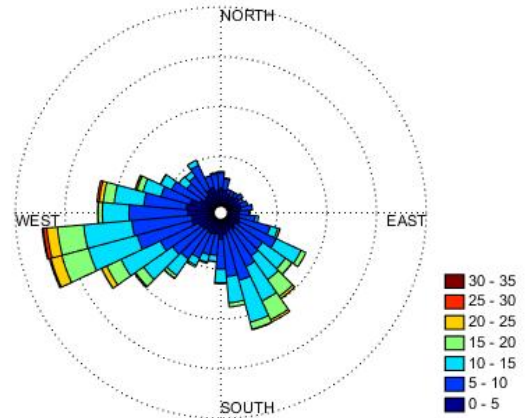


Fig. 5. Wind rose from Roan 328 at 100 m height, the colors indicate wind speed (m/s) given in the legend to the right.

### C. Data Analysis

The pressure at all sites is corrected for height according to ISO 2533 [18], as are the temperature measurements at Roan, assuming a linear variation of the temperature with geopotential altitude. All data from the masts are 10 min. mean values except the pressure and relative humidity data from Sula which are 1 hour averages. At the top height of all three masts there are

two anemometers mounted with an approximate 180° angle between them allowing measurements from the upstream anemometer to be utilized at all times. For the lower heights at Roan where only one anemometer is available, a 45° sector has been filtered out in order to avoid any flow distortion caused by the mast.

1) *Surface boundary layer height*: Monin-Obukhov theory is only valid for uniform horizontal flow within the surface boundary layer [6], which is generally accepted to be the bottom 10% of the planetary boundary layer. Two methods for filtering out the measurements where the surface boundary layer height was below 100 m have here been considered. First, the simple formula of Tennekes [19] was used,

$$z_{sl} = c \frac{u_*}{f}, \quad (6)$$

with  $c = 0.25$  and  $f = 0.0001$ . The expression for the friction velocity is by DNV [13] given to be

$$u_* = \bar{u} \sqrt{\frac{\kappa^2}{(\ln \frac{z}{z_0})^2}}, \quad (7)$$

where  $\kappa = 0.4$ . This method resulted in a threshold value for the friction velocity based on the mean wind speed. The resulting atmospheric stability distribution was lacking results for low wind speeds, and this method was thus discarded.

Although Monin and Obukhov [6] in their theory assume that the fluxes can be considered independent of height in the surface boundary layer, Panofsky [20] found this not to be true and Stull [8] defines the surface layer as the area in which turbulent fluxes and stress vary by less than 10% of their surface values. Using the relationship between the turbulent friction stress and the friction velocity,

$$u_* = \sqrt{\frac{\tau}{\rho}}, \quad (8)$$

the surface boundary layer was defined as the layer in which the friction velocity varies no more than 5% from its value at the surface [21].

Panofsky [20] offers an expression for the correction of the friction velocity with height,

$$u_*(z) = u_{*surface} - 6fz, \quad (9)$$

which is valid for neutral conditions in homogeneous terrain. Equation 7 was used to estimate the surface friction velocity and was extrapolated to 100 m using Equation 9. This approach resulted in large losses of data points; 78% at Roan 328 and 59% at Frøya and Roan 327. The distributions of atmospheric stability however, were found to be very similar before and after filtering. The main difference was a loss in very unstable conditions and less smooth distribution due to the loss in

data points. Weber [14] found that the friction velocity decreases with increasing atmospheric stability. This can imply that for very unstable conditions the friction velocity has a larger decreasing gradient, meaning that a decrease of 5% from its surface value will occur at a lower height for very unstable conditions. This results in a lower surface boundary layer height as the investigations above suggest. The aim of this work is to present representative atmospheric stability distributions at two sites and compare them. Therefore, it is considered a bias when only very unstable conditions are filtered out, and it is decided not to filter for the surface boundary layer height.

## V. COMPARING METHODS

### A. Results

Figure 6 shows the atmospheric stability distribution at Frøya for the surface Richardson method and Figure 7 shows the distribution for the bulk Richardson method. The black curve in the plots shows the amount of data in each bar, given in percent also indicated by the y-axis. The distributions are concurrent and consist of 20542 data points.

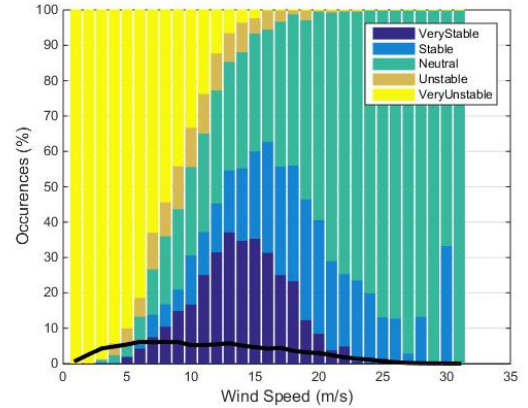


Fig. 6. The surface Richardson method between 100 and 0 m at Frøya.

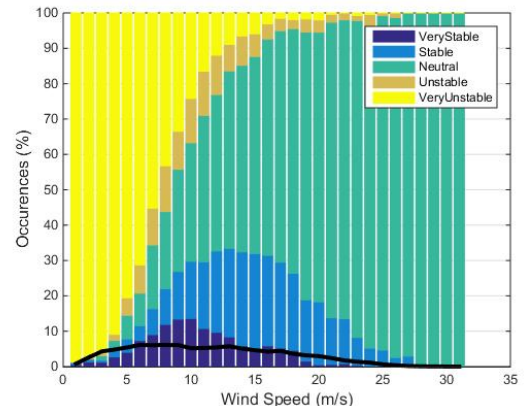


Fig. 7. The bulk Richardson method between 100 and 10 m at Frøya.



The atmospheric stability distributions at Roan 327 are shown in Figures 8, 9 and 10 for the surface Richardson, bulk Richardson and sonic methods, respectively. Only concurrent time steps are plotted, resulting in 13776 data points, starting from April 14 until December 04. The distributions are shown for the comparison between the different methods and are not representative for the area, as the winter months when stable conditions dominate are not present.

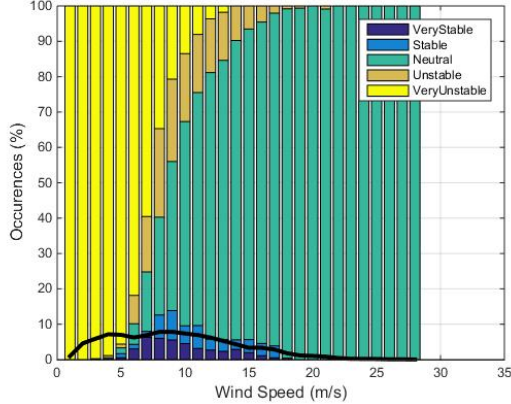


Fig. 8. The surface Richardson method between 100 and 0 m at Roan 327.

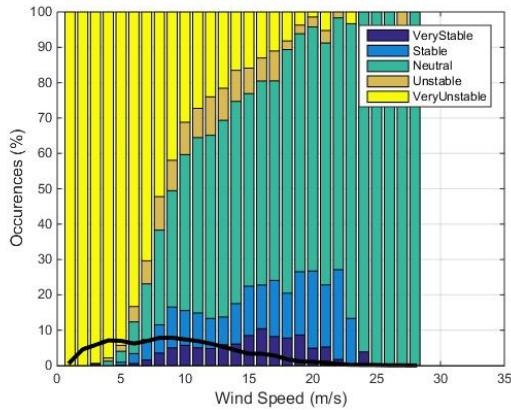


Fig. 9. The bulk Richardson method between 100 and 10 m at Roan 327.

### B. Dependency of accurate measurements

Table III shows an average bulk Richardson number at Roan 327 calculated based on average values of temperature, wind speed, pressure and relative humidity at the site. The average temperature values are then altered within the confines of the accuracy of the temperature measurements, given in Table I, in order to investigate how the Richardson number is affected by worst case inaccuracies. As Table III shows, the Richardson number is very sensitive to changes in temperature. In fact, the value of  $Ri = 0.89$  on row two would be filtered out because Equation 4 is only valid for  $Ri < 0.2$ . Golder [22] comments that the errors in the measurement of the wind at two levels can cause great errors in the

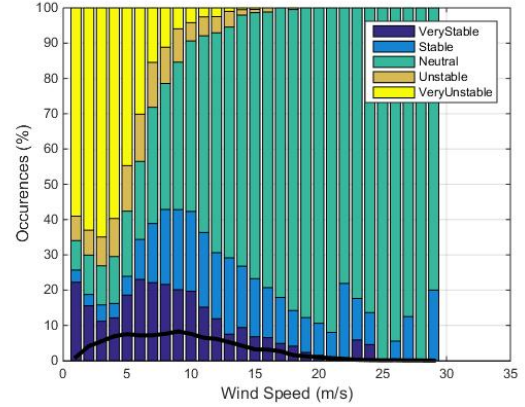


Fig. 10. The sonic method at 98 m at Roan 327.

Richardson number, resulting in a larger scatter for the inaccurately measured data. This shows that the two measuring heights should be as far apart as possible in order for potential inaccuracies in measurements to not affect the results.

TABLE III. UNCERTAINTY ANALYSIS FOR THE MEAN VALUES AT ROAN 327

Temperatures	$\overline{Ri}_{bulk}$
$\overline{T}_2, \overline{T}_1$	-1.64
$\overline{T}_2 + 0.2K, \overline{T}_1 - 0.2K$	0.89
$\overline{T}_2 - 0.2K, \overline{T}_1 + 0.2K$	-4.18

For the data at Roan, the temperature at the bottom height has been linearly corrected to 0 m and 20 m for the surface Richardson and bulk Richardson methods, respectively. The temperature gradient is largest closest to ground [8], [9], and correcting it linearly for height is a rough estimate that leads to large uncertainties, especially because the Richardson number is so dependent of accurate values, as discussed above.

### C. Discussion

The results from Frøya and Roan 327 in Figures 6, 7, 8, 9 and 10 clearly show that the stability distribution for a site varies, depending on which method is chosen to obtain it.

Stable conditions were expected to be predominant close to the ground where the temperature gradient is largest. And the surface Richardson method from Frøya in Figure 6 does show a higher frequency of stable conditions than the bulk Richardson method from Frøya in Figure 7, supporting this hypothesis. It seems that the surface Richardson method displays surface effects that the bulk Richardson method does not convey.

At Roan 327, the surface Richardson method, bulk Richardson method and the sonic method in Figures 8, 9 and 10, respectively, show opposite trends of those at Frøya. This can be due to inaccuracies caused either by the linear correction of the temperature for height or by the measurements. The surface Richardson method in Figure 8 especially shows a unrealistically low frequency

of very stable conditions. The bulk Richardson method in Figure 9 is less affected by the linear correction of height which is most inaccurate closest to ground.

It is interesting to see that the sonic method shows a very similar distribution to the Richardson methods, keeping in mind the curves showing data recovery. The sonic method is valid at 98 m, while the surface Richardson and bulk Richardson are valid at their geometric mean heights  $z_m$ . The lower amount of unstable conditions are thus understandable as the sonic method is valid higher up where the temperature gradient is smaller. However, there are uncertainties related to the temperature derived from sonic anemometers [23], and the temperature from the sonic anemometer mounted at 98m was found to deviate from the values measured by the Galltec Mess KP thermometer mounted at 97 m with approximately +1.5 K. This temperature is used to find the covariance with the vertical wind speed and exposes a weakness in the sonic measurements. In addition, the sonic data were rotated to align the coordinate system to the mean wind, which is reported to be a flawed method, especially in inhomogeneous terrain [14], [24]. The experiences from this measuring campaign are that these anemometers are unstable and expensive. Hence, the sonic method is considered more uncertain than the Richardson methods.

## VI. COMPARING SITES

The atmospheric stability distributions at the three masts are compared in two ways. First, all three masts are compared quantitatively based on representative distributions from each site. This is done because the measurements at Frøya ended before the measuring campaign at Roan started. It also ensures a large amount of data points for each distribution. The bulk Richardson method is chosen for this comparison as the focus of this paper is on large scale wind power, and the surface effects are thus not of interest. Second, the correlation in atmospheric stability is investigated between the two masts at Roan for only concurrent data points.

### A. Results

In Figures 11, 12 and 13 the atmospheric stability distributions at Frøya, Roan 327 and Roan 328 are shown, respectively. Figure 14 shows plots of the very stable, neutral and very unstable conditions at the three sites. The curves for stable and unstable conditions were very similar at all three sites and are thus not compared further.

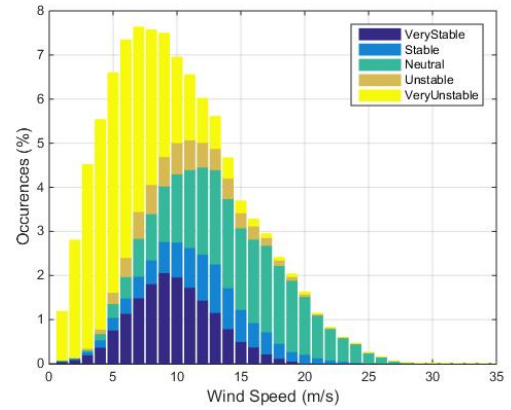


Fig. 11. The atmospheric stability distribution at Frøya. 86256 data points.

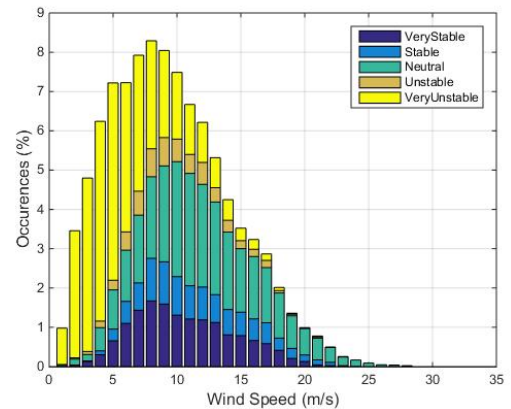


Fig. 12. The atmospheric stability distribution at Roan 327. 27533 data points.

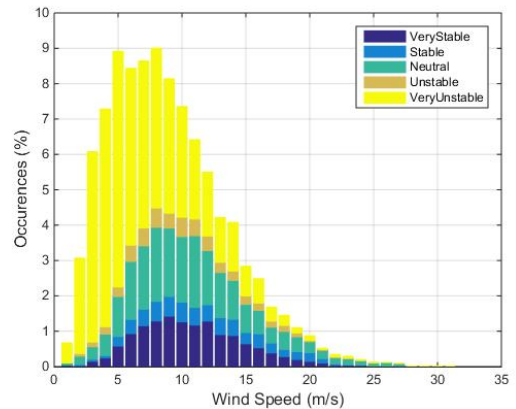


Fig. 13. The atmospheric stability distribution at Roan 328. 19460 data points.

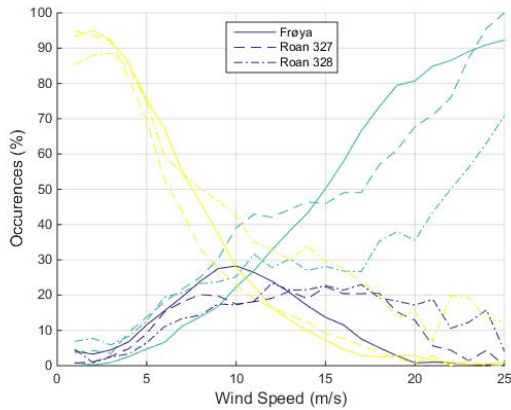


Fig. 14. Comparison of the distributions at the three masts. Yellow shows very unstable, blue very stable and green neutral conditions.

### B. Discussion

The flow over mountains experiences a speed-up effect over the peak, a slight wind speed reduction upstream of the peak and a considerable reduction of the wind speed over the downwind slope of the peak [25], [26]. Zhang [26] found that this speed-up effect was 80% of the undisturbed upstream wind speed, but that these effects are dulled in complex terrain where the topography almost acts like a rough surface [26]. Based on the map in Figure 3 it seems that Roan 328 is located in the area of reduced wind speed prior to a peak when the wind is coming from the south. This causes the mean wind speed to be lower there than at the other sites, as reported in Table II. Furthermore, the map in Figure 3 shows that the wind at Roan 327 has already passed over mountains coming both from the west and the south, resulting in higher wind speeds there than at Roan 328, in accordance with the findings of Zhang [26]. The main wind direction at Frøya is undisturbed flow from the sea, resulting in the highest mean wind speed of the three sites there, as seen in Table II.

The fact that Roan 328 is the site with the lowest mean wind speed and highest mean temperatures result in the highest frequency of unstable conditions for all wind speeds at this site, as Figure 14 shows. This is in accordance with Golder [22] and Panchal and Chandrasekharan [27] who both found that an increase in terrain roughness leads to a shift towards unstable conditions. The higher wind speeds and lower temperatures at Roan 327 lead to weaker heat fluxes at this site, resulting in a higher frequency of neutral conditions.

It is generally understood that winds at sea are stronger and less turbulent than winds on land [28]. Peña et al [2] found neutral conditions to prevail on off shore sites in the North Sea, while stable conditions have been found to be most common at coastal sites [4]. Coelingh et al. [29] found that in the North Sea, the conditions at coastal sites and at off shore platforms compare well for higher wind speeds, above 7 m/s at 10 m height. Heggem [30] researched the stability conditions at Frøya during the winter months and found the conditions there

to be stable, especially for wind speeds below 8 m/s. From the distribution in Figure 11 it thus seems that seasonal trends are present at Frøya for the lower wind speeds, with stable conditions occurring during winter and unstable conditions occurring during summer. For higher wind speeds however, neutral conditions from the sea dominate.

### C. Correlations of atmospheric stability

The two masts at Roan were both measuring in the period 10.12.2014 until 29.11.2015, almost one full year. For this time period, the atmospheric stability at the two masts were compared. When only concurrent time steps were considered, this left 2763 data points for the bulk Richardson method, 1837 data points for the surface Richardson method and 6219 data points for the sonic method to be compared. The following results are thus shown to give a first discussion of the correlation between the two sites, not to be representative for the conditions there.

The comparison is conducted by assigning each stability class a number from 1 (very unstable) to 5 (very stable). The difference between this value at the two masts is then calculated. If the difference is zero, the stability conditions at the two masts are equal, while the difference can maximum be four, meaning the conditions are completely different at the two masts (very unstable and very stable). As Table IV shows, for all three methods it was found that approximately 50% of the occurrences the difference was zero, meaning the two masts were measuring the same stability conditions. It should also be noted from Table IV that the sonic method is the only method resulting in a difference of four between the two sites, which might indicate that this method is less reliable.

TABLE IV. THE FREQUENCY OF OCCURRENCES OF DIFFERENCES BETWEEN THE STABILITY CLASSES AT THE TWO ROAN MASTS

Difference	Bulk Richardson	Surface Richardson	Sonic
0	49%	57%	51%
1	32%	31%	26%
2	18%	11%	14%
3	1%	1%	3%
4	0%	0%	6%

Table V elaborates the findings from Table IV for the bulk Richardson method by specifying the frequency of stability conditions at one mast compared to the other. The blank spaces mean there are no occurrences of that combination of stability classes at the two sites. Table V thus shows that the conditions at the two masts are either both in the stable-neutral or unstable-neutral range. In other words, for these data, the conditions are never unstable at Roan 327 and stable at Roan 328 or vice versa, indicating that the stability conditions at the two sites are correlated. This could be expected as they are situated in the same mountainous area.

TABLE V. THE FREQUENCY OF STABILITY CONDITIONS AT ONE MAST COMPARED TO THE OTHER

		Roan 328				
		Very stable	Stable	Neutral	Unstable	Very unstable
Roan 327	Very stable	11%	6%	7%		
	Stable	3%	3%	6%		
	Neutral	3%	3%	22%	2%	1%
	Unstable			5%	1%	1%
	Very unstable			6%	6%	13%

## VII. CONCLUSION

The Monin-Obukhov theory is only valid under very specific conditions which lead to large amounts of the measured data being filtered out, both in this work and in other works such as Lange [1] and Fechner [3]. Zilitinkevich and Esau [31] comment on this and are motivated to find new models for calculating the fluxes in the atmospheric boundary layer based on resistance and heat-transfer laws. Here, the motivation was not a theoretical one, but to produce representative atmospheric stability distributions for the different sites and to compare them. For this means, filtering for the surface boundary layer height was found not to be necessary as the filtering lead to a bias with loss of very unstable conditions only.

Three methods for calculating atmospheric stability have been compared, namely the bulk Richardson method, the surface Richardson method and the sonic method. It is shown that the resulting stability distributions vary depending on which method is chosen. Although the sonic method at Roan 327 led to a plausible stability distribution, the temperature derived from the sonic anemometer was consequently too high, causing these results to be uncertain, and the Richardson methods to be favored. Which method to apply depends on the area of interest in the atmosphere. If the strong surface effects are of interest, the surface Richardson method should be applied, while for wind power appliances, where the conditions higher in the atmosphere are of interest, the bulk Richardson method is a better choice. It is generally advised to conduct temperature and wind speed measurements at the same height so no correction for height has to be conducted, as this leads to large errors. Furthermore, the two measuring heights should be as far apart as possible to avoid potential errors in the measurements to affect the results.

The representative atmospheric stability distributions at the three sites calculated with the bulk Richardson method were also compared. Roan 328 was the mast with the lowest mean wind speed and highest mean temperatures and thus the site with the highest frequency of very unstable conditions. At Roan 327, there was a higher frequency of strong winds coming from the south, leading to a higher mean wind speed and lower mean temperature, and thus a higher frequency of neu-

tral conditions. At the coastal site Frøya the conditions during high wind speeds were found to be neutral, as is normal over sea. For lower wind speeds, the ocean effects were found not to be decisive for the stability conditions resulting in high frequencies of very stable and very unstable conditions.

Data from the two masts at Roan were collected during a concurrent time period so their distributions could be directly compared. For all three methods it was found that 50% of the time, Roan 327 and Roan 328 experienced the same stability conditions. It was also showed that the conditions at the two masts calculated with the bulk Richardson method were both either stable-neutral or neutral-unstable. This implies that the stability conditions at the two sites were correlated.

The large loss in data points when the concurrent time periods between the Roan masts were considered, arose questions for further work. Firstly, the exercise of comparing the stability classes during concurrent time steps should be repeated when more data points are available. Furthermore, it would be very interesting to be able to describe stability also when  $Ri > 0.2$  as this also leads to large losses in data points. Lastly, authors define the stability classes differently and a common definition should be developed in order to facilitate the comparison of different works.

## ACKNOWLEDGMENT

The author would like to thank Professor Lars Roar Sætran and PhD candidate Lars Morten Bardal for their eager guidance and support throughout the process of this work. In addition, the author is thankful to Meventus for providing data for the Roan masts, in particular John Amund Lund and Anne Simonsen for their enthusiasm and assistance in the processing of the data.

## REFERENCES

- [1] B. Lange, S. Larsen, J. Højstrup, and R. Barthelmie, "The influence of thermal effects on the wind speed profile of the coastal marine boundary layer," *Boundary-Layer Meteorology*, vol. 112, no. 3, pp. 587–617, 2003.
- [2] A. Peña, T. Mikkelsen, S.-E. Gryning, C. B. Hasager, A. N. Hahmann, M. Badger, I. Karagali, and M. Courtney, "Offshore vertical wind shear: Final report on norsewinds work task 3.1," *DTU Wind Energy E No. 0005*, p. 116, 2012.
- [3] Soren Fechner, "Preprocessing of meteorological data for atmospheric theoretical/numerical methods [NTNU master thesis]," 2015.
- [4] R. J. Barthelmie, "The effects of atmospheric stability on coastal wind climates," *Meteorological Applications*, vol. 6, pp. 39–47, 1999.
- [5] S. D. Chambers, F. Wang, A. G. Williams, D. Xiaodong, H. Zhang, G. Lonati, J. Crawford, A. D. Griffiths, A. Ianniello, and I. Allegri, "Quantifying the influences of atmospheric stability on air pollution in lanzhou, china, using a radon-based stability monitor," *Atmospheric Environment*, vol. 107, pp. 233–243, 2015.
- [6] A. Monin and A. Obukhov, "Basic laws of turbulent mixing in the surface layer of the atmosphere," *Tr. Akad. Nauk SSSR Geophys. Inst.*, vol. 24, pp. 163–187, 1954.
- [7] S. P. Arya, "Finite-difference errors in estimation of gradients in the atmospheric surface layer," *Journal of Applied Meteorology*, vol. 30, no. 2, pp. 251–253, 1991.

- [8] R. B. Stull, *An Introduction to Boundary Layer Meteorology*. Kluwer Academic Publishers, 1988, vol. 13.
- [9] S. E. Larsen, *Observing and Modelling the Planetary Boundary Layer*, ser. Nato ASI Series. Springer Berlin Heidelberg, 1993, vol. 5.
- [10] D. W. Byun, "On the analytical solution of flux-profile relationships for the atmospheric surface layer," *Journal of Applied Meteorology*, vol. 29, pp. 652–657, 1990.
- [11] A. J. Dyer, "A review of flux-profile relationships," *Boundary-Layer Meteorology*, vol. 7, no. 3, pp. 363–372, 1974.
- [12] J. A. Businger, J. C. Wyngaard, Y. Izumi, and E. F. Bradley, "Flux-profile relationships in the atmospheric surface layer," *Journal of the Atmospheric Sciences*, vol. 28, no. 2, pp. 181–189, 1971.
- [13] Det Norske Veritas, "Recommended Practice DNV-RP-C205 Environmental Conditions and Environmental Loads," pp. 14–23, 2010. [Online]. Available: <https://rules.dnvgl.com/docs/pdf/DNV/codes/docs/2010-10/RP-C205.pdf>
- [14] R. O. Weber, "Remarks on the definition and estimation of friction velocity," *Boundary-Layer Meteorology*, vol. 93, no. 2, pp. 197–209, 1999.
- [15] Ingunn Sletvold Øistad, "Site analysis of the Titran Met-masts [NTNU project thesis]," 2014.
- [16] The Norwegian Mapping Authority. [Online]. Available: <http://www.kartverket.no/en/>
- [17] D. E. Weir, *Vindkraft - Produksjon i 2013*. Norges vassdrags- og energidirektorat, 2014.
- [18] International organization for standardization, Switzerland, "International Standard ISO 2533 Standard Atmosphere," pp. 1–6, 1975. [Online]. Available: [standard.no](http://www.iso.org)
- [19] H. Tennekes, *Similarity Relations, Scaling Laws and Spectral Dynamics*. Springer Netherlands, 1982.
- [20] H. A. Panofsky, *Tower Micrometeorology, Ch 4 in Workshop on Micrometeorology*, D. A. Haugen, Ed. American Meteorology Society, Boston, MA, 1973.
- [21] S.-E. Gryning, E. Batchvarova, B. Brmmmer, H. Jørgensen, and S. Larsen, "On the extension of the wind profile over homogeneous terrain beyond the surface boundary layer," *Boundary-Layer Meteorology*, vol. 124, no. 2, pp. 251–268, 2007.
- [22] D. Golder, "Relations among stability parameters in the surface layer," *Boundary-Layer Meteorology*, vol. 3, pp. 47–58, 1972.
- [23] P. Schotanus, F. Nieuwstadt, and H. de Bruin, "Temperature measurement with a sonic anemometer and its application to heat and moisture fluxes," *Boundary-Layer Meteorology*, vol. 26, pp. 81–93, 1983.
- [24] F. K. Chow, S. F. D. Wekker, and B. J. Snyder, Eds., *Mountain Weather Research and Forecasting - Recent Progress and Current Challenges*, ser. Springer Atmospheric Sciences. Springer Netherlands, 2013, vol. 5.
- [25] S. Emeis, *Wind Energy Meteorology - Atmospheric Physics for Wind Power Generation*, ser. Green Energy and Technology. Springer Berlin Heidelberg, 2013.
- [26] M. H. Zhang, *Wind Resource Assessment and Micro-siting: Science and Engineering*. John Wiley and Sons Singapore Pte Ltd, 2015.
- [27] N. S. Panchal and E. Chandrasekharan, "Terrain roughness and atmospheric stability at a typical coastal site," *Boundary-Layer Meteorology*, vol. 27, pp. 89–96, 1983.
- [28] J. P. Coelingh, A. J. M. van Wijk, and A. A. M. Holtslag, "Analysis of wind speed observations over the north sea," *Journal of Wind Engineering and Industrial Aerodynamics*, vol. 61, pp. 51–69, 1996.
- [29] —, "Analysis of wind speed observations on the north sea coast," *Journal of Wind Engineering and Industrial Aerodynamics*, vol. 73, pp. 125–144, 1998.
- [30] Tore Heggem, "Measurements of Coastal Wind and Temperature -Sensor Evaluation, Data Quality, and Wind Structures [NTNU doctor scientarium thesis]," 1997.
- [31] S. S. Zilitinkevich and I. N. Esau, "Resistance and heat-transfer laws for stable and neutral planetary boundary layers: Old theory advanced and re-evaluated," *Q. J. R. Meteorological Society*, vol. 131, pp. 1863–1892, 2005.